Radial Flow of Dust Particles in Accretion Disks [1]

Taku Takeuchi and D. N. C. Lin
UCO/Lick Observatory, University of California, Santa Cruz, CA95064

ABSTRACT

We study the radial migration of dust particles in accreting protostellar disks analogous to the primordial solar nebula. Our main objective is to determine the retention efficiency of dust particles which are the building blocks of the much larger planetesimals. This study takes account of the two dimensional (radial and normal) structure of the disk gas, including the effects of the variation in the gas velocity as a function of distance from the midplane. It is shown that the dust component of disks accretes slower than the gas component. At high altitude from the disk midplane (higher than a few disk scale heights), the gas rotates faster than particles because of the inward pressure gradient force, and its drag force causes particles to move outward in the radial direction. Viscous torque induces the gas within a scale height from the disk midplane to flow outward, carrying small (size $\lesssim 100$ μm at 10 AU) particles with it. Only particles at intermediate altitude or with sufficiently large sizes ($\gtrsim 1$ mm at 10 AU) move inward. When the particles' radial velocities are averaged over the entire vertical direction, particles have a net inward flux. The magnitude of their radial motion depends on the particles' distance from the central star. At large distances, particles migrate inward with a velocity much faster than the gas accretion velocity. However, their inward velocity is reduced below that of the gas in the inner regions of the disk. The rate of velocity decrease is a function of the particles' size. While larger particles retain fast accretion velocity until they approach closer to the star, 10 μm particles have slower velocity than the gas in the most part of the disk ($r \lesssim 100$ AU). This differential migration of particles causes the size fractionation. Dust disks composed mostly of small particles (size $\lesssim 10$ μm) accrete slower than gas disks, resulting in the increase in the dust-gas ratio during the gas accretion phase. If the gas disk has a steep radial density gradient or if dust particles sediment effectively to the disk midplane, the net vertically averaged flux of particles can be outward. In this case, the accretion of the dust component is prevented, leading to the formation of residual dust disks after their gas component is severely depleted.

Subject headings: accretion, accretion disks — planetary systems: formation — solar system: formation

1. Introduction

Planets form in circumstellar disks. In the standard scenario, formation of earth-size planets or planetary cores occurs through coagulation of small dust particles (e.g., Weidenschilling & Cuzzi 1993). Thus, the total amount, radial density distribution, and size distribution of dust particles in the disks are the important initial conditions of planet formation. In many of the previous studies of planet formation, the dust-gas ratio of circumstellar disks is assumed to be similar to the solar value ($\sim 10^{-2}$), and dust particles are considered to be well mixed with gas, i.e., the dust-gas ratio is constant throughout the disk (Hayashi, Nakazawa, & Nakagawa 1985).

However, the motion of dust particles is different from that of gas. Dust particles have a radial motion which is induced by the gas drag force. Adachi, Hayashi, & Nakazawa (1976) and Weidenschilling (1977) studied the motion of particles in gas disks. Due to radially outward pressure gradient force, the rotation velocity of the gas is gen-

[1] To appear in Dec. 20 issue of Astrophys. J.

erally slower than particles on nearly Keplerian circular orbits. Consequently, the gas drag force takes angular momentum from particles, resulting in their inward migration (Whipple 1972). At a few AU from the central star, the orbital decay time is estimated to be $\sim 10^6$ yr for 100 μm particles and 10^4 yr for 1 cm particles. These times are much shorter than the life time of gas disks ($\sim 10^7$ yr). Thus, dust component may evolve much faster than the gas in protostellar disks, in which case, the dust-gas ratio would decline. It appears that the initial conditions of planet formation need not to be protostellar disks in which dust particles are well mixed with the gas and the dust-gas ratio is constant.

In this paper, we start a series of studies to determine the initial distribution of dust particles in the context of planet formation. Here, we study the radial migration of dust particles in gas disks. We focus our attention on particles smaller than ~ 1 cm in order to consider evolution of dust disks before the initiation of planetesimal formation. The migration of these small particles establishes the initial density distribution of the dust component and sets the stage for planetesimal formation. In this phase of disk evolution, the gas component is considered to be turbulent and is accreting onto the star. The discussion in the above paragraph is based on the study of particle migration under the assumption that particles have completely sedimented on the midplane of laminar disks. However, in turbulent disks, the sedimentation of particles is prevented, because particles are stirred up to high altitude from the midplane by turbulent gas motion. In such disks, particles are distributed in the vertical direction, and the radial motion of particles depends on the distance from the midplane. Thus, there is a need for studying the radial migration of particles which reside above the midplane.

There are two important factors causing the vertical variation in the migration velocity of particles. The first is the variation of rotation velocity of the gas in the vertical direction. As mentioned above, the gas rotation differs from the Keplerian rotation because of the gas pressure gradient. As the gas density decreases with the distance from the midplane, the radial pressure gradient varies and under some circumstances even changes its sign. While at the midplane the pressure gradient force is outward, it is inward near the disk surface because the disk thickness increases with the radius. The gas drag force on particles also varies with the height, resulting in a variation of particle migration velocities. In §3.1, we will see that particles at high altitude, where the pressure gradient force is inward, flow outward.

The second factor is the variation in the radial gas flow. Small particles ($\lesssim 100$ μm) are well coupled to the gas, so that they migrate with the gas flow, as discussed in §3.1 below. That is if the gas is accreted onto the star, the small particles would also be accreted, while if the gas flows outward, particle flow would also be outward. In accreting protostellar disks, the gas does not always flow radially inward. Radial velocity of the gas varies with the distance from the midplane. Viscous stress can cause gas outflow near the midplane (Urpin 1984; Kley & Lin 1992). Różyczka, Bodenheimer, & Bell (1994) showed that the outflow occurs if the radial pressure gradient at the midplane is steep enough. The density (or pressure) gradient at the midplane is steeper than the average spatial (or surface) density gradient, e.g., if the surface density varies as $\Sigma_g \propto r^{-1}$ and the disk thickness varies as $h_g \propto r$, the midplane density has a steeper variation corresponding to $\rho_g \propto r^{-2}$. Viscous diffusion at the midplane causes the outflow of the gas to reduce the steep density gradient. On the other hand, at high altitude from the midplane, the density gradient is shallow and the viscous torque causes the usual inward flow. Thus, in accretion disks, the outward flow at the midplane is sandwiched by the inflow at the disk surfaces (see §2.2 for details). Because small particles are carried by the gas flow, they are expected to flow outward near the midplane, and inward at higher altitude.

Thus, if most of dust particles concentrate in the region where they migrate outward, i.e., near the disk surface or around the midplane, the dust component of the disk would accumulate in total mass and expand in size. In reality, the vertical spatial distribution of particles is determined by the degree of sedimentation, and their size distribution is regulated by the coagulation, condensation, and sublimation processes. In this paper, we calculate the vertical distribution of particles in order to identify the mass flux of the dust particles as functions of their size and their distance from

the midplane and their host stars. The results of the present calculation will be used to study the long term dynamical evolution of the dust component of the disk. For the present task, we do not consider the effects of gas depletion, particles' size evolution or their feedback influence on the flow velocity of the gas. These effects will be considered in a future investigation.

There are several works on the particle migration in turbulent disks. Stepinski & Valageas (1997) derived the vertically averaged velocity of migration for two limiting cases. One model is constructed for small particles which are well mixed with the gas and the other is for large particles which are totally sedimented to the midplane. The velocity for intermediate sized particles is calculated by the interpolation of these limiting cases. Supulver & Lin (2000) investigated the evolution of particle orbits in turbulent disks numerically. This paper gives analytical expression of the particle velocity for any size of particles, which are estimated from interpolation by Stepinski & Valageas (1997). Several studies showed that vortices or turbulent eddies can trap particles within some size range (Barge & Sommeria 1995; Cuzzi, Dobrovolskis, & Hogan 1996; Tanga et al. 1996; Klahr & Henning 1997; Cuzzi et al. 2001, see however Hodgson & Brandenburg 1998). Particle trapping by eddies may be important for local collection of size-sorted particles. In this paper, turbulent eddies are treated just as a source of the particle diffusion and of the gas viscosity. The effect of particle trapping on their coagulation is not discussed here.

The plan of the paper is as follows. In §2, the vertical variation of gas flow is derived. In §3, we describe how the radial velocity of dust particles varies in the vertical direction, and then calculate the net radial migration velocity. In §4, we discuss the steady distribution of particles assuming no particle growth. We show that the size fractionation of particles occurs as a result of radial migration, and that the distribution of particles differs from that of the gas.

2. Viscous Flows of Gas Disks

2.1. Rotation Law of the Gas

Gas disks rotate with a slightly different velocity from the Keplerian velocity. The rotation velocity is determined by the balance between the stellar gravity, the centrifugal force, and the gas pressure gradient. In cylindrical coordinates (r, z), the balance of the forces described by the momentum equation in the r-direction is given by

$$r\Omega_g^2 - \frac{GMr}{(r^2+z^2)^{3/2}} - \frac{1}{\rho_g}\frac{\partial P_g}{\partial r} = 0 \ , \qquad (1)$$

where Ω_g is the angular rotation velocity of the gas, G is the gravitational constant, M is the stellar mass, ρ_g is the gas density, and P_g is the gas pressure. The density distribution in the vertical direction is determined by the balance between the z-components of the stellar gravity and the pressure gradient, which is written as

$$-\frac{GMz}{(r^2+z^2)^{3/2}} - \frac{1}{\rho_g}\frac{\partial P_g}{\partial z} = 0 \ . \qquad (2)$$

We assume that the disk is isothermal in the vertical direction. Neglecting $(z/r)^2$ and higher order terms, the vertical density distribution is obtained as

$$\rho_g(r,z) = \rho_g(r,0)\exp\left(-\frac{z^2}{2h_g^2}\right) \ . \qquad (3)$$

The disk scale height h_g is given by

$$h_g(r) = \frac{c}{\Omega_{\rm K,mid}} \ , \qquad (4)$$

where c is the isothermal sound speed, and $\Omega_{\rm K,mid} = \sqrt{GM/r^3}$ is the Keplerian angular velocity at the midplane. The radial variations of physical quantities are assumed to have power law forms, such that

$$\begin{aligned} \rho_g(r,z) &= \rho_0 r_{\rm AU}^p \exp\left(-\frac{z^2}{2h_g^2}\right) \ , \\ c^2(r) &= c_0^2 r_{\rm AU}^q \ , \\ h_g(r) &= h_0 r_{\rm AU}^{(q+3)/2} \ , \end{aligned} \qquad (5)$$

where the subscript "0" means the values at 1 AU, $r_{\rm AU}$ is the radius in the unit of AU, and power law indices p and q are usually negative. The surface density is

$$\Sigma_g(r) = \int_{-\infty}^{+\infty} \rho_g dz = \sqrt{2\pi}\rho_0 h_0 r_{\rm AU}^{p_s} \ , \qquad (6)$$

where $p_s = p + (q+3)/2$. To derive the rotation law of the gas, we retain $(z/r)^2$ and lower order

terms in equation (1), then obtain

$$\Omega_g(r,z) = \Omega_{\rm K,mid}\left[1+\frac{1}{2}\left(\frac{h_g}{r}\right)^2\left(p+q+\frac{q}{2}\frac{z^2}{h_g^2}\right)\right] . \quad (7)$$

The difference of the gas rotation from the Kepler rotation is order of $(h_g/r)^2$, and the gas at high altitude rotates slower than the gas at the midplane.

2.2. Radial Velocity of the Gas Flow

In viscous disks, angular momentum is transfered from the inner part to the outer part of the disk under the action of viscous stress. The azimuthal component of the momentum equation implies

$$2\pi r\rho_g\left(v_{r,g}\frac{\partial}{\partial r}+v_{z,g}\frac{\partial}{\partial z}\right)(r^2\Omega_g) = 2\pi\left[\frac{\partial}{\partial r}\left(r^3\rho_g\nu\frac{\partial\Omega_g}{\partial r}\right)+\frac{\partial}{\partial z}\left(r^3\rho_g\nu\frac{\partial\Omega_g}{\partial z}\right)\right] , \quad (8)$$

where $v_{r,g}$ and $v_{z,g}$ are the r- and z-components of the gas velocity, respectively, and ν is the kinetic viscosity. The right hand side of equation (8) represents the torque exerted on an annulus with unit width in the r- and z-directions. The left hand side is the variation of the angular momentum of the annulus accompanying with the motion. We assume that the angular velocity is always adjusted to the equilibrium (eq. [7]) on a dynamical time scale. Since molecular viscosity is too ineffective, it is customary to assume that angular momentum is primarily transported by the Reynolds stress induced by the turbulent motion of the gas. Following conventional practice, we adopt an *ad hoc* but simple to use α prescription for turbulent viscosity (Shakura & Sunyaev 1973), such that

$$\nu = \alpha c h_g = \alpha c_0 h_0 r_{\rm AU}^{q+3/2} . \quad (9)$$

The mass conservation of the gas is

$$\frac{\partial\rho_g}{\partial t}+\frac{1}{r}\frac{\partial}{\partial r}(r\rho_g v_{r,g})+\frac{\partial}{\partial z}(\rho_g v_{z,g}) = 0 . \quad (10)$$

In accretion disks considered here, the second term is the same order of the third term. Then, we see that $v_{z,g} \sim (h_g/r)v_{r,g}$. Besides, from equation (7) we see $\partial(r^2\Omega_g)/\partial z \sim (h_g/r)\partial(r^2\Omega_g)/\partial r$. Thus, $v_{z,g}\partial(r^2\Omega_g)/\partial z$ is factor $(h_g/r)^2$ smaller than $v_{r,g}\partial(r^2\Omega_g)/\partial r$ and can be neglected in equation (8). Using power law expressions (5) and (9) and retaining terms of order $(h_g/r)^2$, the radial velocity is reduced to

$$v_{r,g} = -2\pi\alpha\left(\frac{h_0}{\rm AU}\right)^2\left(3p+2q+6+\frac{5q+9}{2}\frac{z^2}{h_g^2}\right) \times r_{\rm AU}^{q+1/2}\ {\rm AU\ yr^{-1}} . \quad (11)$$

In the following discussions, we adopt these values as being representative of a typical model: $M = 1M_\odot$, $\rho_0 = 2.83\times10^{-10}$ g cm^{-3}, $h_0 = 3.33\times10^{-2}$ AU, $p = -2.25$, $q = -0.5$, and $\alpha = 10^{-3}$. These values correspond to a minimum mass solar nebula whose surface density distribution has a power law form with index $p_s = p+(q+3)/2 = -1.0$ and has a gas mass $2.5\times10^{-2}M_\odot$ inside 100AU.

Figure 1 shows the radial velocity of the gas. The radial velocity is outward (positive) near the midplane, while it is inward (negative) above the height $0.73h_g$. In the standard model ($q=-0.5$), the radial velocity is independent of the distance from the star, as seen from equation (11). At the midplane, the radial gradient of the gas density is so steep ($p=-2.25$) that the gas receives more torque from the inner disk than the torque it exerts on the outer disk. This radial dependence means that viscous stress acts to move the gas outward in such a steep density gradient. The condition for the outward gas flow at the midplane is

$$p+\frac{2}{3}q < -2 , \quad (12)$$

which is satisfied in many accretion disk models. The rotation of the gas is slower at higher altitude as seen in equation (7). Thus, the gas at the midplane loses its angular momentum through the action of viscous stress it has with the gas at higher altitude. However, in the standard model, this angular momentum loss is smaller than the angular momentum gain through the viscous stress in the r-direction. The outflow zone around the midplane shrinks as the radial density gradient is reduced ($p\to0$), and when the condition (12) is violated, gas at all altitudes flows inward. The radial density gradient is shallower at higher altitude, because the disk scale height increases with the radius. Thus, at high altitude, the gas loses more angular momentum through exerting torque

on the outer disk than it is receiving from the inner disk. For such gas, the presence of viscous torque induces it to flow towards the star.

The net radial velocity of the gas is given by averaging in the vertical direction:

$$\begin{aligned}\langle v_{r,g}\rangle &= \frac{1}{\Sigma_g}\int_{-\infty}^{+\infty} v_{r,g}\rho_g dz \\ &= -6\pi\alpha\left(\frac{h_0}{\mathrm{AU}}\right)^2 (p_s+q+2) \\ &\quad \times r_{\mathrm{AU}}^{q+1/2}\ \mathrm{AU\ yr^{-1}}\ . \end{aligned} \quad (13)$$

The net accretion of the gas toward the star occurs if

$$p_s + q = p + \frac{3}{2}(q+1) > -2\ . \quad (14)$$

We may consider two models in which a steady state is achieved. One model is the case in which the net radial velocity is zero, i.e., $p_s+q=-2$. For example, if $p_s=-1.5$ and $q=-0.5$, there is no net accretion of the disk. A more realistic model is the case in which the mass flux of the gas is constant with the radius, i.e., $r\Sigma_g\langle v_{r,g}\rangle \propto r^{p_s+q+3/2}$ is constant. We take this as our standard model, i.e., $p_s=-1.0$ and $q=-0.5$. This surface density profile is expected to arise after the disk has undergone a period of initial viscous evolution.

3. Radial Flow of Dust Particles

3.1. Vertical Dependence of Radial Velocity

The azimuthal velocities of dust particles are different from that of the gas. The resulting gas drag force transfers angular momentum between the particles and the gas and moves particles in the radial direction. If there is no gas drag force, particles would orbit with the Keplerian angular velocity, which is approximated as

$$\Omega_{\mathrm{K}}(r,z) \approx \Omega_{\mathrm{K,mid}}\left(1-\frac{3}{4}\frac{z^2}{r^2}\right)\ . \quad (15)$$

We express the deviation of the angular velocity of the gas from the Keplerian angular velocity as

$$\Omega_g = \Omega_{\mathrm{K}}(1-\eta)^{1/2}\ . \quad (16)$$

From equation (1) it is seen that $\eta = -(r\Omega_{\mathrm{K}}^2\rho_g)^{-1}\partial P_g/\partial r$ is the ratio of the gas pressure gradient to the stellar gravity in the radial direction. From equations (7), (15), and (16), η is written within the order of $(h_g/r)^2$ as,

$$\eta = -\left(\frac{h_g}{r}\right)^2\left(p+q+\frac{q+3}{2}\frac{z^2}{h_g^2}\right)\ . \quad (17)$$

Note that the pressure gradient force is outward (η is positive) around the midplane, while it is inward (η is negative) where $|z| > \sqrt{-2(p+q)/(q+3)}h_g$. In the standard model, η changes sign at $z \approx 1.5h_g$. Dust particles near the midplane rotate faster than the gas, and particles at high altitude rotate slower than the gas.

The equations of motion of a particle are

$$\frac{dv_{r,d}}{dt} = \frac{v_{\theta,d}^2}{r} - \Omega_{\mathrm{K}}^2 r - \frac{\Omega_{\mathrm{K,mid}}}{T_s}(v_{r,d}-v_{r,g})\ , \quad (18)$$

$$\frac{d}{dt}\left(rv_{\theta,d}\right) = -\frac{v_{\mathrm{K,mid}}}{T_s}(v_{\theta,d}-v_{\theta,\mathrm{g}})\ , \quad (19)$$

where v_r and v_θ are the r- and θ- components of the velocity, respectively, with the subscripts "g" and "d" distinguishing gas and dust, and $v_{\mathrm{K,mid}} = r\Omega_{\mathrm{K,mid}}$ is the Keplerian velocity at the midplane. The gas drag force is expressed through the non-dimensional stopping time T_s (normalized by the Kepler time at the midplane). We do not solve the equation of motion in the z-direction. Instead, we simply assume $v_{z,d}=0$. When an equilibrium in the vertical dust distribution is achieved, the dust sedimentation to the midplane is balanced by the diffusion of particles, as discussed below in §3.2. The vertical velocity of a particle is zero when time averaged.

The mean free path of gas molecules is larger than 1 cm for $r \gtrsim 1$ AU in our models (Nakagawa, Sekiya, & Hayashi 1986). In this paper, we consider particles smaller than 1 cm and use Epstein's gas drag law. Then, the non-dimensional stopping time T_s, as given by Takeuchi & Artymowicz (2001), is

$$T_s = \frac{\rho_p s v_{\mathrm{K,mid}}}{\rho_g r v_T}\ , \quad (20)$$

where ρ_p is the particle internal density, s is the particle radius, and the mean thermal velocity is $v_T = \sqrt{8/\pi}c$ [2]. We take the particle internal density as $\rho_p = 1.25$ g cm^{-3}.

[2] In Takeuchi & Artymowicz (2001), v_T is defined to be 4/3 times the mean thermal velocity. This definition causes a factor 4/3 difference between equation (20) and their equation (10).

For particles smaller than 1 cm, the non-dimensional stopping time is much smaller than unity through most of the disk. Figure 2 shows the radii of particles whose stopping time is unity. At the midplane (see the solid line), the non-dimensional stopping time is smaller than unity for particles of size $s \lesssim 1$ cm at $r \lesssim 100$ AU. At $z = 2h_g$ (the dashed line), although the gas density is lower than at the midplane and the stopping time is longer, particles of size $s \lesssim 1$ mm still have the non-dimensional stopping time smaller than unity. These particles are well coupled to the gas and their angular velocity is similar to the gas angular velocity (7). Only particles with $s \gtrsim 1$ cm which are located at high altitude and $r \gtrsim 100$ AU become decoupled from the gas.

We assume that motions of both the gas and the particles are close to Keplerian, i.e., $v_{\theta,g} \approx v_{\theta,d} \approx v_{\rm K,mid}$, and that $d(rv_{\theta,d})/dt \approx v_{r,d} d(rv_{\rm K,mid})/dr = v_{r,d} v_{\rm K,mid}/2$. Then, from equation (19), we have

$$v_{\theta,d} - v_{\theta,g} = -\frac{1}{2} T_s v_{r,d} \ . \tag{21}$$

Using equation (16) and neglecting terms of order $(h_g/r)^4$ and higher, equation (18) is reduced to

$$\frac{dv_{r,d}}{dt} = -\eta \frac{v_{\rm K,mid}^2}{r} + \frac{2v_{\rm K,mid}}{r}(v_{\theta,d} - v_{\theta,g}) - \frac{\Omega_{\rm K,mid}}{T_s}(v_{r,d} - v_{r,g}) \ . \tag{22}$$

The left hand side is order of $v_{r,d}^2/r$ and is neglected if $v_{r,d} \ll c$. Substituting equation (21) into equation (22), we find the radial velocity of the particle to be

$$v_{r,d} = \frac{T_s^{-1} v_{r,g} - \eta v_{\rm K,mid}}{T_s + T_s^{-1}} \ . \tag{23}$$

In the above derivation of the particle's radial velocity, we assume that in the z-direction the particle sedimentation is balanced by the turbulent diffusion, but that in the r-direction the turbulent effects are neglected.

For particles well coupled with the gas ($T_s \ll 1$), the radial velocity reduces to

$$v_{r,d} = v_{r,g} + v_{r,\rm drift} \ , \tag{24}$$

where $v_{r,\rm drift} = -\eta T_s v_{\rm K,mid}$ is the relative velocity from the gas. Using equations (5), (17), and (20),

$$v_{r,\rm drift} = 2\pi \left(\frac{h_0}{\rm AU}\right)^2 \left(p + q + \frac{q+3}{2}\frac{z^2}{h_g^2}\right) \times r_{\rm AU}^{q+1/2} T_{s,\rm mid} \exp\left(\frac{z^2}{2h_g^2}\right) \ {\rm AU\ yr^{-1}} \ , \tag{25}$$

where $T_{s,\rm mid}$ is the non-dimensional stopping time at the midplane. The radial drift velocity increases exponentially with the height. Because the particles are strongly coupled with the gas, the gas drag force suppresses their drift velocity. At the midplane where the gas density is highest, the suppression of the drift is most effective. The drift velocity at the midplane is

$$v_{r,\rm drift,mid} = \sqrt{\frac{\pi^3}{2}} \frac{h_0 s}{\rm AU^2} \frac{\rho_p}{\rho_0} (p+q) r_{\rm AU}^{-p+q/2-1} \ {\rm AU\ yr^{-1}} \ , \tag{26}$$

which agrees with the derivations of Adachi et al. (1976) and Weidenschilling (1977).

For large particles decoupled from the gas ($T_s \gg 1$), the radial motion of the gas does not affect the particles' velocity, so that $v_{r,d} = -\eta T_s^{-1} v_{\rm K,mid}$. In this paper, we do not consider such large particles.

Figure 3 shows the radial velocity $v_{r,d}$ of particles of $s = 10$ μm, 100 μm, and 1 mm at 10 AU in the standard model disk. Near the midplane, the drift velocity $v_{\rm drift}$ (relative to the gas velocity shown by the dotted line) of 10 μm particles is small. The particles move outward almost together with the gas. As the altitude increases and the gas velocity decreases, the radial velocity of the particles also decreases, then becomes negative. At $z \approx 1.5h_g$ where η changes its sign, the radial pressure gradient vanishes and the gas rotates with the Keplerian velocity. The particles co-rotate with the gas at that location, and have the same radial velocity as the gas. The drift velocity changes its sign to become positive. At high altitude ($z \gtrsim 2h_g$) where the gas drag is weak, the particles' drift velocity begins to increase rapidly, and then the radial velocity becomes positive again at $z \gtrsim 3h_g$. The behavior of the radial velocity of 100 μm particles is qualitatively similar to that of 10 μm particles, i.e., it is outward at the midplane, inward at intermediate altitude, and outward again at high altitude. The coupling of 100 μm particles to the gas is weaker,

so that their radial velocity is much different from the gas velocity even at the midplane. However, the drift velocity at the midplane is still slightly smaller than the gas outflow velocity and the particles move outward. Particles of 1 mm move inward even at the midplane, because the inward drift velocity of such large particles is larger than the outflow velocity of the gas. These large particles also move outward at high altitude where the gas rotates faster than the particles.

3.2. Vertical Distribution of Particles

At the beginning stage of star formation from molecular cloud cores, dust particles in circumstellar disks may be well mixed with the gas and the dust-gas ratio may be uniform throughout the disk. After the termination of gas infall onto the disks, the disks become to be hydrostatic and particles begin to sediment toward the midplane because of the z-component of the stellar gravity. The particles reach the terminal velocity, where the gravity and the gas drag balance with each other,

$$v_{z,d} = -\Omega_{\rm K,mid} T_s z \ . \tag{27}$$

The time scale of the sedimentation is $t_{\rm sed} \sim z/v_{z,d} \sim T_s^{-1}\Omega_{\rm K}^{-1}$. If this time scale is much smaller than the radial migration time scale, $t_r \sim r/v_{r,d} \sim (\alpha + T_s)^{-1}(h_g/r)^{-2}\Omega_{\rm K}^{-1}$, i.e., if $T_s/\alpha \gg (h_g/r)^2$, then the particles sediment before the large migration in the r-direction. (At high altitudes or around the midplane, particles may drift to the opposite direction to the gas, as seen in Fig. 3. Some particles with $T_s \sim \alpha$ may have the radial migration time scale t_r much larger than the above estimate. Even for such particles, the condition $T_s/\alpha \gg (h_g/r)^2$ for the fast sedimentation is still valid.) For example, at 10 AU in a disk with $\alpha = 10^{-3}$ and $(h_g/r)^2 \sim 10^{-3}$, particles larger than 0.2 μm sediment to the midplane without large radial movement.

We consider disks at later stages, such as the T Tauri stage. The disks are still turbulent, and the turbulent motion of the gas stirs dust particles up to high altitude to prevent dust sedimentation. An equilibrium distribution of particles in the vertical direction is achieved by the balance between the sedimentation and the diffusion due to the turbulent gas.

The turbulent diffusion is modeled in an analogy of molecular diffusion, provided that the particles are considered to be the passive tracers of fluid, i.e., if the particles have no influence on the gas motion and have the similar velocity of the surrounding gas [see e.g., chapter 10 in Monin & Yaglom (1971) and section 3.5.1 in Morfill (1985)]. The equation of continuity is written as

$$\frac{\partial}{\partial t}\rho_d + \nabla\cdot(\rho_d \boldsymbol{v}_d + \boldsymbol{j}) = 0 \ , \tag{28}$$

where ρ_d is the particle density, and $\boldsymbol{v}_d$ is the particle velocity. The diffusive mass flux $\boldsymbol{j}$ is estimated by

$$\boldsymbol{j} = -\frac{\rho_g \nu}{\rm Sc}\nabla\left(\frac{\rho_d}{\rho_g}\right) \ , \tag{29}$$

where the Schmidt number Sc represents the strength of coupling between the particles and the gas. For small particles, Sc approaches unity and the particles have the same diffusivity as the gas, while it becomes infinite for large particles. For intermediate particle sizes, Sc can be as small as 0.1, which means that particle diffusion occurs effectively (see e.g., Fig. 1 in Cuzzi et al. 1993). In our standard model, we use Sc = 1. If Sc is not unity, the particles are not the passive tracers which completely follow the fluid motion. In this case, the formulation according to the analogy of molecular diffusion may be inappropriate. In addition, if the velocity of sedimentation, $v_{z,d}$, is comparable to or larger than the turbulent velocity, the particle could not be the passive tracers. The estimate of the diffusive mass flux by equation (29) should be considered just as a "gradient diffusion hypothesis."

In a steady state of axisymmetrical disks, $\partial/\partial t$ and $\partial/\partial\theta$ in equation (28) is zero. In addition, for particles satisfying the condition $T_s/\alpha \gg (h_g/r)^2$ (i.e., for particles sedimenting fast without large radial migration), we see that $\partial(\rho_d v_{z,d})/\partial z \gg \partial(\rho_d v_{r,d})/\partial r$. Therefore, the mass flux in the z-direction must be zero, i.e.,

$$\rho_d v_{z,d} - \rho_g \frac{\nu}{\rm Sc}\frac{\partial}{\partial z}\left(\frac{\rho_d}{\rho_g}\right) = 0 \ . \tag{30}$$

This equation is the same as the one derived by Dubrulle, Morfill, & Sterzik (1995). Solving equation (30) with equations (3), (4), (9), (20), and

(27) gives the particle density

$$\rho_d(r,z) = \rho_d(r,0) \exp\left[-\frac{z^2}{2h_g^2} - \frac{\mathrm{Sc} T_{s,\mathrm{mid}}}{\alpha} \left(\exp\frac{z^2}{2h_g^2} - 1 \right) \right] . \quad (31)$$

The first term in the exponential comes from the gas distribution and the second term represents the sedimentation. In the limit of tight coupling of the particles and the gas ($T_{s,\mathrm{mid}} = 0$), the particle distribution is the same as that of the gas. The surface mass density of dust particles is

$$\Sigma_d(r) = \int_{-\infty}^{+\infty} \rho_d(r,z) dz . \quad (32)$$

Figure 4*a* shows variation of the dust-gas ratio in the vertical direction at 10 AU in the standard model disk. We see the sedimentation of particles. [3] Large particles ($\gtrsim 1$ mm) sediment around the midplane, while small particles ($\lesssim 10$ μm) spread over a few scale height of the gas disk. These small particles are stirred up to high altitude by the turbulence of the gas. The gas drag force becomes weaker at higher altitude where the gas density decreases, so the gas cannot sustain the dust particles there. Thus, the particle density drops rapidly at some altitude and the dust disk obtains a relatively sharp surface (e.g., at $z \sim 2.5 h_g$ for 10 μm particles). The sedimentation of particles is more effective in the outer part of the disk, farther away from the star (see Fig. 4*b*). For example, 100 μm particles at 1 AU spread over the gas disk, while the particles at 100 AU concentrate around the midplane. At the outer part of the disk, the gas density is lower, so that the gas drag is weaker and turbulence cannot loft the particles to high altitudes.

Dust particles are well mixed with the gas if

$$\frac{\mathrm{Sc} T_{s,\mathrm{mid}}}{\alpha} \left(\exp\frac{z^2}{2h_g^2} - 1 \right) \ll 1 , \quad (33)$$

i.e., below the height

$$\frac{z}{h_g} = \left[2 \log\left(\frac{\alpha}{\mathrm{Sc} T_{s,\mathrm{mid}}} + 1 \right) \right]^{1/2} . \quad (34)$$

[3] We obtained slightly thinner distribution of particles than that by Dubrulle et al. (1995) which is shown in their Figure 3. They assumed that the stopping time of particles, which is inversely proportional to the gas density, to be constant and used the value at the midplane. This assumption causes the dust disk to puff out.

In the standard model, particles smaller than

$$s \ll 20\ r_{\mathrm{AU}}^{-1}\ \mu\mathrm{m} \quad (35)$$

uniformly distribute with regard to the gas under the height $z = 3h_g$.

3.3. Net Radial Velocity

As discussed in §3.1, the radial velocity of particles varies with the altitude. In this subsection, we discuss the net radial velocity averaged in the vertical direction.

3.3.1. Particles Well Mixed with the Gas

At the beginning stage of formation of circumstellar disks, small particles would be distributed uniformly in the disk gas. Before the particles have undergone enough sedimentation, their net radial velocity averaged in the vertical direction is

$$\langle v_{r,d} \rangle = \frac{1}{\Sigma_g} \int_{-\infty}^{+\infty} \rho_g v_{r,d} dz . \quad (36)$$

Figure 5 shows the net radial velocities of small particles. The velocity of particles approaches the gas velocity as the distance from the star becomes smaller. Near the star, the gas density is high enough to induce almost all particles to move together with the gas. As the distance from the star increases, the gas density decreases and particles at high altitude begin to drift outward from the gas. At sufficiently large distance from the star, the net radial velocity can be positive, i.e., particles move outward. However, before they move over a large distance in the radial direction, they also sediment to the midplane. The time scale of the outward radial motion is $t_{\mathrm{out}} \sim r/\langle v_{r,d} \rangle \sim 1/(\eta T_s \Omega_{\mathrm{K}})$ (for outflowing particles, $|v_{r,g}|$ is smaller than $|v_{r,\mathrm{drift}}|$ and is neglected in the estimate of t_{out}), while the sedimentation time scale is $t_{\mathrm{sed}} \sim z/v_{z,d} \sim 1/(T_s \Omega_{\mathrm{K}})$. Because $\eta \ll 1$, $t_{\mathrm{out}} \gg t_{\mathrm{sed}}$. The outward motion of those particles which are well mixed with the gas may proceed shortly after the formation of circumstellar disks, but it does not significantly modify the radial distribution of dust particles. The evolution of radial distribution occurs primarily through the motion of sedimented particles.

3.3.2. Removal of Outflow at High Altitude by the Sedimentation

The net radial velocity of sedimented particles is

$$\langle v_{r,d} \rangle = \frac{1}{\Sigma_d} \int_{-\infty}^{+\infty} \rho_d v_{r,d} dz \ . \qquad (37)$$

The function $\rho_d v_{r,d}/\Sigma_d$, which is proportional to the mass flux, is shown in Figure 6. Because of the sedimentation to the midplane, which is efficient for larger particles, the mass flux is dominated by the particles near the midplane. For example, the mass flux of 10 μm particles is mainly carried by particles moving outward around the midplane ($|z| \lesssim 0.7 h_g$) and by those moving inward at intermediate altitude ($0.7 h_g \lesssim |z| \lesssim 2.9 h_g$). Although particles at high altitude ($|z| \gtrsim 2.9 h_g$) move outward, their contribution to the mass flux is negligibly small. Very large particles, for example 1 mm particles, move inward even at the midplane. Thus, the sedimentation causes the vast majority of particles to move inward.

Sedimentation effectively removes outflowing particles at high altitude. This flow pattern is seen as follows. The particles flowing outward have a drift velocity larger than the gas inflow velocity, i.e., $|v_{r,\mathrm{drift}}| > |v_{r,g}|$. From equations (11) and (25), it is seen that $\alpha^{-1} T_{s,\mathrm{mid}} \exp(z^2/2h_g^2) \gtrsim 1$ for such particles. However, from equation (31), we also see that the density of these particles is as small as $\rho_d(z)/\rho_d(0) \lesssim e^{-1}$. Therefore, very few particles remain in the outflow region at high altitude.

If the sedimentation is so effective that most particles concentrate around the midplane ($|z| \lesssim h_g$), e.g., for particles larger than 1 mm at 10 AU (see Fig. 4*a*), the inward drift velocity at the midplane is larger than the gas outflow velocity. Thus, such particles flow inward. Again from equation (31), we see that $T_{s,\mathrm{mid}}/\alpha \gtrsim 1$ for such particles. Then, it is seen from equations (11) and (25) that $|v_{r,\mathrm{drift}}| \gtrsim |v_{r,g}|$ at the midplane. This inequality implies that when particles grow up sufficiently large sizes to sediment toward and to concentrate around the midplane, they become decoupled from the outflow motion of the gas. If the sedimentation is so efficient that all particles concentrate in a thin layer at the midplane ($T_{s,\mathrm{mid}}/\alpha \gg 1$), the radial motion of the particles would not affected by the radial motion of the gas. In this limit, the particles' motion is similar to that deduced by Adachi et al. (1976) and Weidenschilling (1977).

3.3.3. Net Velocity of Sedimented Particles

Figure 7*a* shows the net radial velocities of sedimented particles. These net radial velocities are negative for particles of all sizes. Particles rapidly move inward when they are at large distances from the star. In the outer regions of the disk, particles sediment and concentrate at the midplane, and their net radial velocity, which is much faster than the gas outflow velocity $v_{r,g}$, is approximated by the drift velocity at the midplane (eq. [26]). Their inward velocity decreases as they approach the star, because the suppression of inward velocity by the gas drag becomes stronger. The time scale of their orbital decay is $r/\langle v_{r,d} \rangle \propto r^{2+p-q/2}$. When they approach the location where the gas density is dense enough to make $T_{s,\mathrm{mid}}/\alpha \lesssim 1$, the inward drift velocity becomes smaller than the gas outflow velocity at the midplane. The particles begin to move with the gas flow. At the same time, particles are spreaded over more than the disk scale height. The particles' net radial velocity approaches the net gas velocity (the dashed line in Fig. 7*a*). However, because the particle distribution concentrates slightly more to the midplane than the gas distribution, the number of particles riding on the outflowing gas around the midplane is larger than in the case where the particle distribution is same as the gas. The enhancement of outflowing particles retards their net inflow velocity to values below that of the gas. At the inner part of the disk, the net inward velocity of particles is always slower than the gas velocity. Near the star, the particles mix more with the gas and their motion converges with that of the gas. The particles' inward velocity has a minimum magnitude, $\langle v_{r,d} \rangle = 5.2 \times 10^{-6}$ AU/yr, which is about half of the gas velocity. Particles smaller than 10 μm have a slower inward velocity than the gas throughout nearly the entire disk ($r \lesssim 100$ AU), while particles larger than 1 mm have slower velocity only in the innermost part of the disk ($r \lesssim 1$ AU). The difference in the inward velocity induces the size fractionation of particles, as discussed in §4.1 below. The dust-gas ratio may increase during the viscous evolution of disks, because the accretion velocity of small particles is slower than that of the gas.

Small particles which satisfy the condition (35) are mixed well with the gas. The net radial velocities of such small particles may be calculated by equation (36), even after larger particles have undergone the sedimentation. It is seen from comparison between Figures 5 and 7*a* that, e.g., for 10 μm particles, the radial velocities are about the same in both figures for $r \lesssim 1$ AU, while they deviate significantly between these figures for $r \gtrsim 10$ AU. As shown in Figure 5, the radial velocity of 10 μm particles at $r \gtrsim 10$ AU is outward when the particles are mixed with the gas, i.e., in the very first stage of disk formation. However, after the particle sedimentation, the radial velocity becomes inward even at $r \gtrsim 10$ AU, as shown in Figure 7*a*. It is concluded that the particle sedimentation suppresses the outward flow of particles in the standard model.

3.3.4. Various Models

In Figure 7*b*, we show the case with $p_s = -0.5$ where the surface density profile of the gas is flatter than in the standard model. The velocity profiles are qualitatively similar to those in the standard model. Particles of 10 μm move slower than the gas throughout nearly the entire disk, while 1 mm particles rapidly migrate inward.

In Figure 7*c*, the case with a steeper surface density gradient is shown. In this model, we adopt $p_s = -1.3$ which satisfies the condition (14) for inward gas accretion flow. In this case, we see that the net radial velocity of particles becomes positive at some locations. In these regions, the accretion of particles is prevented. The particles flowing inward from large distances terminate their migration at the location where the net radial velocity becomes zero, and then accumulate at that particular orbital radius. Particles located just inside this critical radius flow outward and accumulate there also. Particles at the innermost part of the disk flow inward onto the star. Size fractionation occurs because the location of the accumulation depends on the particle size. The accumulation continues as particles drift radially inward from large radii until particles in the outer disk are significantly depleted or the number density of accumulated particles becomes so high that the removal of particles through coagulation or collisional destruction becomes efficient. Although accretion of dust particles terminates at some locations, the gas disk continues to accrete onto the star. The dust-gas ratio increases as the accretion of the gas proceeds.

3.3.5. Self-similarity of the Velocity Profile

The functions of net radial velocities shown in Figure 7 for various sizes have self-similar forms. From equations (11), (24), (25), (31), (32), and (37), the net radial velocity can be written as

$$\langle v_{r,d} \rangle = 2\pi\alpha \left(\frac{h_0}{\mathrm{AU}} \right)^2 r_{\mathrm{AU}}^{q+1/2} F\left(p, q, \mathrm{Sc}; \frac{T_{s,\mathrm{mid}}}{\alpha} \right) \ \mathrm{AU\ yr^{-1}}\ , \tag{38}$$

where F is a function of p, q, Sc, and $T_{s,\mathrm{mid}}/\alpha$,

$$F\left(p, q, \mathrm{Sc}; \frac{T_{s,\mathrm{mid}}}{\alpha} \right) = \int_{-\infty}^{+\infty} \left\{ -3p - 2q - 6 - (5q+9) z'^2 + \left[p + q + (q+3) z'^2 \right] \frac{T_{s,\mathrm{mid}}}{\alpha} \exp z'^2 \right\} \times \exp\left[-z'^2 - \frac{\mathrm{Sc} T_{s,\mathrm{mid}}}{\alpha} \left(\exp z'^2 - 1 \right) \right] dz' \times \left\{ \int_{-\infty}^{+\infty} \exp\left[-z'^2 - \frac{\mathrm{Sc} T_{s,\mathrm{mid}}}{\alpha} \left(\exp z'^2 - 1 \right) \right] dz' \right\}^{-1} \tag{39}$$

and $z' = z/\sqrt{2}h_g$. If we vary the properties of particles, keeping $T_{s,\mathrm{mid}}/\alpha$ to be constant, the function F yields the same value. For example, when we vary the particle size $s \to s'$, then transform the orbital radius as $r \to r' = (s'/s)^{1/[p+(q+3)/2]} r$, we have the same value of $T_{s,\mathrm{mid}}/\alpha$ and the same functional form of F. In our models, $q = -1/2$, so $\langle v_{r,d} \rangle$ depends on r only through the function F. In this case, the profiles of the net radial velocities for different sizes are obtained by the transformation in the r-direction from one profile. In Figure 8, the function F is plotted for various values of the Schmidt number Sc.

3.3.6. Various Schmidt Numbers

In the standard model, the net radial velocity of particles is inward everywhere in the disk. This flow pattern is partially due to the removal of particles, through sedimentation, from high altitudes where they would flow outward. For particles which are sufficiently large to concentrate near the midplane, the magnitude of their inward drift velocity is larger than that of the outflowing gas. Thus, the strength of the sedimentation is always moderate enough to remove outflowing

particles. The sedimentation is controlled by coupling of particles to the turbulent motion of the gas. If coupling is relatively strong (Sc is smaller than unity), the sedimentation would be less effective and particles would mix more completely to the gas, while if it is relatively weak (Sc is larger), particles would concentrate more to the midplane. Usually Sc is assumed to be unity, but the actual value may be different from unity. Some experimental data are plotted in Figure 1 in Cuzzi et al. (1993) which show Sc as small as 0.1 when the Stokes number St is about 0.01 (the Stokes number is considered to be the same order of the non-dimensional stopping time T_s in our models). For large particles (St $\sim T_s \gtrsim 1$), Sc increases with the particle size.

Figure 7*d* shows the net radial velocities in the case where the sedimentation is efficient (Sc = 10). The net radial velocity becomes outward at its peak. Thus, an accumulation of particles and an increase in the dust-gas ratio would occur. Because of the strong sedimentation, the dust disk is much thinner than in the standard model (Sc = 1) and concentrates more to the midplane where the gas flows outward. In the outer part of the disk (for example $r \gtrsim 10$ AU for 100 μm particles), the inward drift velocity of particles (relative to the gas) at the midplane is faster than the outward gas velocity. As the particles drift in, the inward velocity decreases, and at some distances from the star ($r \sim 10$ AU for 100 μm particles), the inward drift velocity at the midplane becomes smaller than the outward gas velocity, and the particles around the midplane flow outward. At such distances, the dust disk is still concentrated around the midplane, and the net radial velocity is dominated by the particles around the midplane and is outward. As the distance from the star decreases, the particles mix more with the gas and the concentration to the midplane becomes weaker. The net radial velocity approaches the gas velocity, which is inward, at the innermost part of the disk.

If the Schmidt number Sc is less than unity, the sedimentation of particles is less efficient. Therefore, the particles are always well mixed with the gas at where the inward drift velocity of particles is smaller than the gas outflow velocity (i.e., at where the particle outflow at the midplane occurs). Thus, the net radial velocity of particles is inward everywhere.

Figure 8 shows the function F for various values of the Schmidt number, Sc = 0.1, 1, and 10. The net radial velocity has the same sign as F (see eq. [38]). It is seen that the outflow of dust particles occurs if the sedimentation is efficient (Sc $\gtrsim 10$).

4. Discussion and Summary

4.1. Steady Density Distribution of Dust Particles

Because the inward velocity of particles depends on their size, particles of different sizes accumulate at different locations. In this subsection, we discuss the density distribution of dust particles as a consequence of their radial flow and show how their size fractionation may occur. We adopt the models in which the net velocity of particles is always inward (Sc = 1 and $p_s \geq -1.0$). We assume that the distribution of particles approaches a steady state after a brief stage of initial evolution. When a steady state is achieved, the mass flux of dust particles becomes constant in the radial direction. We calculate the mass flux of particles as

$$\frac{d\dot{M}_d}{ds} = 2\pi r \langle v_{r,d} \rangle \frac{d\Sigma_d}{ds} \ , \tag{40}$$

where $\dot{M}_d$ and Σ_d are the mass flux and the surface density, respectively, of particles smaller than size s. For simplicity, we neglect three physical processes. First, the evolution of the particle size through the coagulation, collisional destruction, condensation, and sublimation is neglected, i.e., we assume the mass flux $d\dot{M}_d/ds$ for each size range is constant in the radial direction. Second, in turbulent disks, the particles' mass flux comes not only from the mean flow with an average velocity $\langle v_{r,d} \rangle$ but also from the turbulent diffusion of particles, which appears as $\boldsymbol{j}$ in equation (28) for example. We neglect the mass flux from the turbulent diffusion. Third, we assume the structure of the gas component of the disk is entirely determined by the gas itself. We neglect the feedback drag induced by the particles on the gas. In the limit that the spatial density of the dust component becomes comparable to that of the gas near the midplane, this effect would speed up the azimuthal velocity of the gas to the Keplerian value and quench the radial migration of the dust (Cuzzi et al. 1993). Such a dust concentration requires substantial sedimentation of relatively large parti-

cles. Contributions from all of these factors will be investigated in future grain-evolution calculations. Here, we adopt the simplest assumptions to focus on showing the size fractionation of particles. The mass flux of particles in all size range is

$$\dot{M}_{d,\mathrm{all}} = \int_{s_{\min}}^{s_{\max}} \frac{d\dot{M}_d}{ds} ds \ , \tag{41}$$

where $s_{\min}$ and $s_{\max}$ are the minimum and maximum sizes of particles, respectively. The surface density in the steady state is calculated from equation (40) with given $\dot{M}_d$. Figure 9*a* shows the surface density of the dust component composed of single size particles. Particles of different sizes have different density profiles. If the dust component is composed of relatively large particles, it would be concentrate at the inner region of the disk. Thus, as particles grow in size, their surface density distribution becomes more centrally concentrated. Figure 9*b* shows the surface density, assuming the size distribution of particles is a power law with index -3.5, $s_{\min} = 0.1$ μm, and $s_{\max} = 10$ cm. The surface density distribution of the dust particles is different from that of the gas. The power law index of the dust distribution Σ_d is about -1.5 for a gas disk with index $p_s = -1.0$ (-1.2 for a gas disk with $p_s = -0.5$). The implied power law index, -1.5, is similar to the value anticipated from the present mass distribution of planets in the solar system (Hayashi et al. 1985). However, note that the density distributions in Figure 9 are derived assuming no size evolution of particles, and no turbulent diffusion in the radial direction. The growth of particles during the radial flow adds a source term in the equation of continuity. The evolution of the dust density profile should be investigated further by taking particle growth and turbulent diffusion into account.

4.2. Evolution of the Dust-gas Ratio

The accretion velocity of dust particles is different from that of the gas. This difference causes evolution of the dust-gas ratio. In the standard model, 10 μm particles between 10 and 100 AU have an inflow velocity which is about half of the gas velocity. Thus, if the mass of the dust disk is dominated by 10 μm particles (for example, if the particles have size distribution $n \propto s^{-3.5}$ with maximum size 10 μm), the dust-gas ratio would increase through the gas accretion. For example, if the initial mass of the gas disk is $0.11 M_\odot$ and it reduces to $0.01 M_\odot$ after viscous accretion, the dust-gas ratio would increase to be 6 times of its initial value. The increase in the dust-gas ratio speeds up the formation of planetesimals through mutual collisions. Their enhanced abundance may also cause the dust component to become unstable and promote the planetesimal formation through the gravitational instability (Goldreich & Ward 1973; Sekiya 1998).

If the particle growth proceeds to make 1 mm to 1 cm particles during the gas accretion phase, such large particles migrate inward rapidly and accumulate in the inner part of the disk (see Fig 9*a*). This size fractionation causes an increase in the dust-gas ratio at the inner disk, while this process may decrease the dust-gas ratio at the outer disk, resulting in a dust disk concentrated to the inner part of the gas disk.

4.3. Summary

The radial migration of dust particles in accretion disks is studied. Our results are as follows.

1. Dust particles move radially both inward and outward by the gas drag force. Particles at high altitude ($|z| \gtrsim 2h_g$) move outward because they rotate slower than the gas whose pressure gradient force is inward. Small particles ($s \lesssim 100$ μm at 10 AU) near the midplane ($|z| \lesssim h_g$) are advected by the gas outflow. On the other hand, particles at intermediate altitude and large particles ($s \gtrsim$ 1 mm at 10 AU) move inward.

2. The net radial velocity, averaged in the vertical direction, is usually inward, provided that the radial gradient of the gas surface density is not too steep ($p_s \gtrsim -1.3$). Sedimentation removes outflowing particles from high altitudes. Small particles, which can be advected by the outflowing gas around the midplane, do not concentrate at the midplane. In the inner part of the gas disk ($r \lesssim 100$ AU for 10 μm particles), the inflow velocity of particles is smaller than the gas accretion velocity, resulting in an increase in the dust-gas ratio.

3. The particle sedimentation would be efficient if dust-gas coupling is relatively weak (Sc > 1.0). If the sedimentation is so efficient (Sc $\gtrsim 10$), the number of outflowing particles around the mid-

plane would be large, and the direction of the net radial velocity of particles would change to outward at some distances from the star. Accumulation of particles at such locations serves to increase the local dust-gas ratio.

4. The inflow velocity of particles depends on the particle size. Therefore, the inflow causes the size fractionation of particles. Larger particles accumulate at distances closer to the star.

We are grateful to the anonymous referee who gave us important criticism, especially on the improper treatment of particle diffusion in the original version of the manuscript. His/her suggestions also considerably improved the paper. We thank Greg Laughlin for careful reading of the manuscript and Jeff Cuzzi for discussions on the turbulent motion of dust particles. This work was supported in part by an NSF grant AST 99 87417 and in part by a special NASA astrophysical theory program that supports a joint Center for Star Formation Studies at UC Berkeley, NASA-Ames Research Center, and UC Santa Cruz.

REFERENCES

[Adachi et al. 1976]Adachi, I., Hayashi, C., & Nakazawa, K. 1976, Prog. Theor. Phys. 56, 1756

[Barge & Sommeria 1995]Barge, P., & Sommeria, J. 1995, A&A, 295, L1

[1]Cuzzi, J. N., Dobrovolskis, A. R., & Champney, J. M. 1993, Icarus, 106, 102

[Cuzzi et al. 1996]Cuzzi, J. N., Dobrovolskis, A. R., & Hogan, R. C. 1996, in Chondrules and the Protoplanetary Disk, ed. R. H. Hewins, R. H. Jones, & E. R. D. Scott (Cambridge:Cambridge Univ. Press), 35

[Cuzzi et al. 2001]Cuzzi, J. N., Hogan, R. C., Paque, J. M., & Dobrovolskis, A. R. 2001, ApJ, 546, 496

[Dubrulle et al. 1995]Dubrulle, B., Morfill, G., & Sterzik, M. 1995, Icarus, 114, 237

[Goldreich & Ward 1973]Goldreich, P., & Ward, W. R. 1973, ApJ, 183, 1051

[2]Hayashi, C., Nakazawa, K., & Nakagawa, Y. 1985, in Protostars and Planets II, ed. D. C. Black & M. S. Matthews (Tucson:Univ. of Arizona Press), 1100

[Hodgson & Brandenburg 1998]Hodgson, L. S., & Brandenburg, A. 1998, A&A, 330, 1169

[Klahr & Henning 1997]Klahr, H. H., & Henning, T. 1997, Icarus, 128, 213

[3]Kley, W., & Lin, D. N. C. 1992, ApJ, 397, 600

[4]Monin, A. S., & Yaglom, A. M. 1971, Statistical Fluid Mechanics: Mechanics of Turbulence, Volume 1 (Cambridge: The MIT Press), Ch. 10

[5]Morfill, G. E. 1985, in Birth and Infancy of Stars, eds. R. Lucas, A. Omont, & R. Stora (Amsterdam: Elsevier Science Publishers), 693

[6]Nakagawa, Y., Nakazawa, K., & Hayashi, C. 1981, Icarus, 45, 517

[7]Nakagawa, Y., Sekiya, M., & Hayashi, C. 1986, Icarus, 67, 375

[8]Różyczka, M., Bodenheimer, P., & Bell, K. R. 1994, ApJ, 423, 736

[9]Sekiya, M. 1998, Icarus, 133, 298

[10]Shakura, N. I., & Sunyaev, R. A. 1973, A&A, 24, 337

[Stepinski & Valageas 1997]Stepinski, T. F., & Valageas P. 1997, A&A, 319, 1007

[Supulver & Lin 2000]Supulver, K. D., & Lin, D. N. C. 2000, Icarus, 146, 525

[Tanga et al. 1996]Tanga, P., Babiano, A., Dubrulle, B., & Provenzale, A. 1996, Icarus, 121, 158

[Takeuchi & Artymowicz 2001]Takeuchi, T., & Artymowicz, P. 2001, ApJ, 557, 990

[Urpin 1984]Urpin, V. A. 1984, Soviet Astron., 28, 50

[Weidenschilling 1977]Weidenschilling, S. J. 1977, MNRAS, 180, 57

[Weidenschilling & Cuzzi 1993]Weidenschilling, S. J., & Cuzzi, J. N. 1993, in Protostars and Planets III, ed. E. H. Levy & J. I. Lunine (Tucson:Univ. of Arizona Press), 1031

[Whipple 1972]Whipple, F. L. 1972, in From Plasma to Planet, ed. A. Elvius, (London:Wiley), 211

AAS LaTeX macros v5.0.

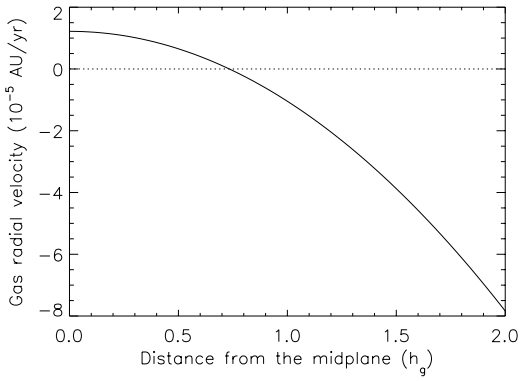

Fig. 1.— Radial velocity of gas $v_{r,g}$. The distance from the midplane z is normalized by the disk scale height h_g. In the standard model ($q = -0.5$), the radial velocity is independent of the distance from the star. The dotted line shows the zero velocity for reference.

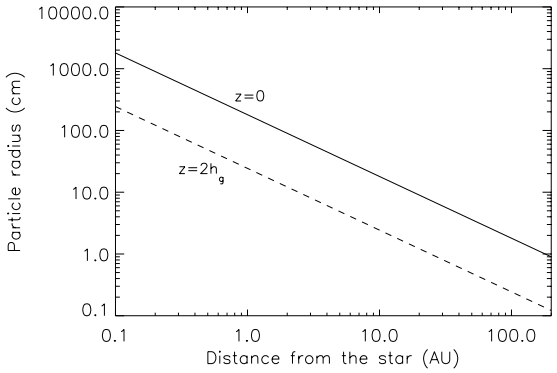

Fig. 2.— The particle radius whose non-dimensional stopping time T_s is unity in the standard disk ($p_s = -1.0$ and $q = -0.5$). The solid line corresponds to particles at the midplane, while the dashed line corresponds to particles at altitude $z = 2h_g$. Particles smaller than the lines have T_s smaller than unity and couple well with the gas, while particles larger than the lines have $T_s > 1$.

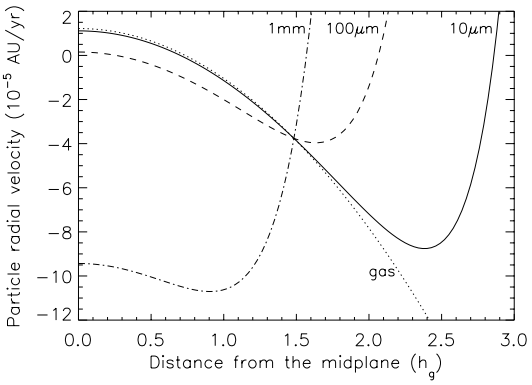

Fig. 3.— Radial velocity $v_{r,d}$ of dust particles of $s = 10$ μm (solid line), 100 μm (dashed line), and 1 mm (dot-dashed line) at 10 AU. The distance from the midplane z is normalized by the disk scale height $h_g = 0.59$ AU. The dotted line shows the radial velocity of the gas $v_{r,g}$.

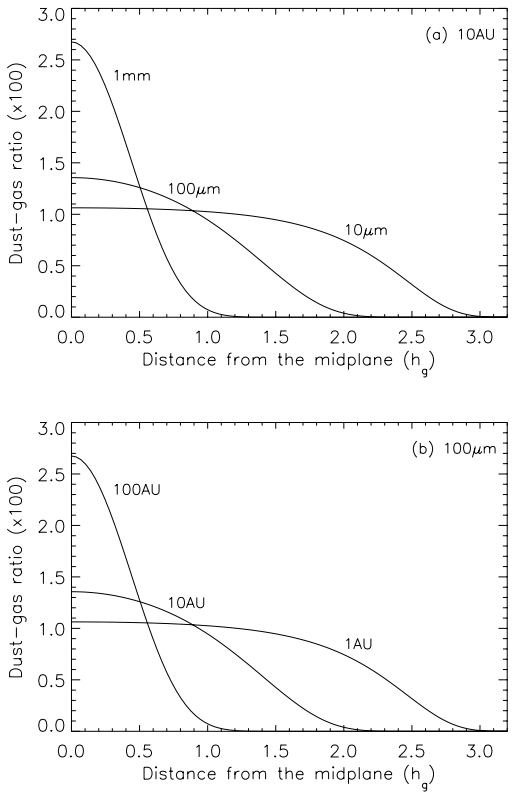

Fig. 4.— Dust-gas ratio, ρ_d/ρ_g, against the distance from the midplane (a) for various sizes at 10 AU and (b) at various locations for 100 μm. The distance from the midplane z is normalized by the disk scale height h_g. The averaged dust-gas ratio is assumed to be 0.01. (a) Three solid lines show the dust-gas ratio of particles of 1 mm, 100 μm, and 10 μm from the left line. (b) Three solid lines show the dust-gas ratio at 100 AU, 10 AU, and 1 AU from the left line.

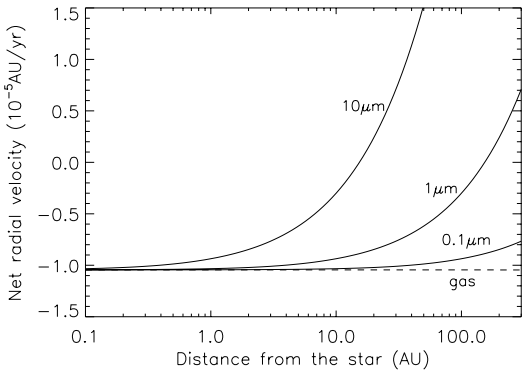

Fig. 5.— Net radial velocity of particles well mixed with the gas, $\langle v_{r,d} \rangle$. The three solid lines correspond to $s = 10$ μm, 1 μm, and 0.1 μm particles from the upper line. The dashed line shows the gas accretion velocity.

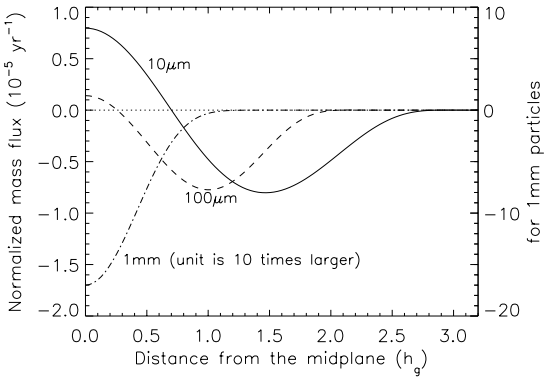

Fig. 6.— Normalized mass flux $\rho_d v_{r,d}/\Sigma_d$ at 10 AU. The solid, dashed, and dot-dashed lines are for $s = 10$ μm, 100 μm, and 1 mm particles, respectively. For 1 mm particles (dot-dashed line), 1/10 of the value is plotted (or refer the ordinate at the right hand side). The distance from the midplane z is normalized by the disk scale height $h_g = 0.59$ AU. The dotted line shows the zero velocity for reference.

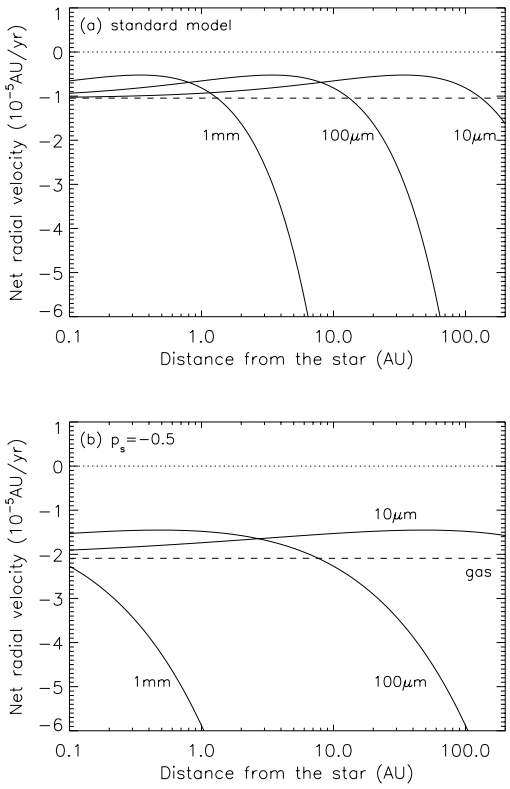

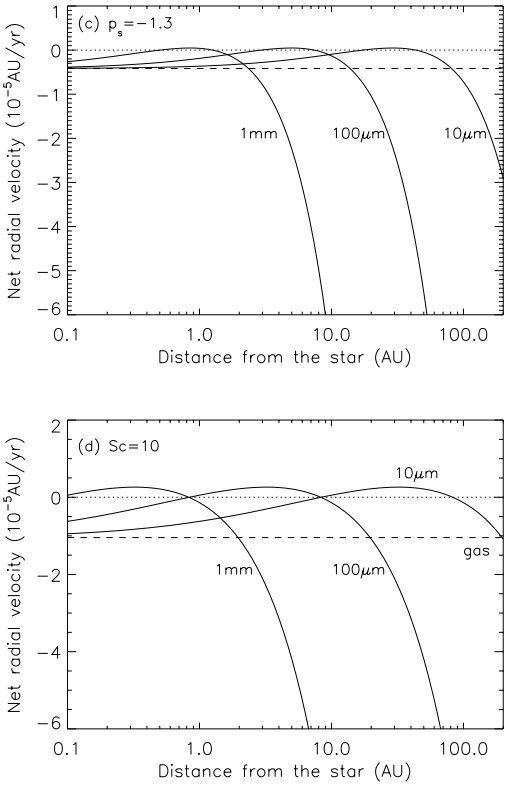

Fig. 7.— Net radial velocity $\langle v_{r,d} \rangle$ of sedimented particles. Three solid lines correspond to $s = 1$ mm, 100 μm, and 10 μm particles from the left line. The accretion velocity of the gas is shown by the dashed line, and the dotted line shows the zero velocity for reference. (a) the standard model ($p_s = -1.0$, $q = -0.5$, and Sc = 1.0) (b) $p_s = -0.5$. (c) $p_s = -1.3$. (d) Sc = 10.

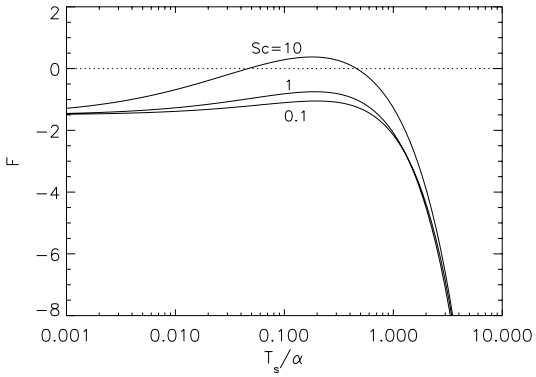

Fig. 8.— Function F for various values of the Schmidt number, Sc = 10, 1, and 0.1 from the upper line. The dotted line shows the zero for reference.

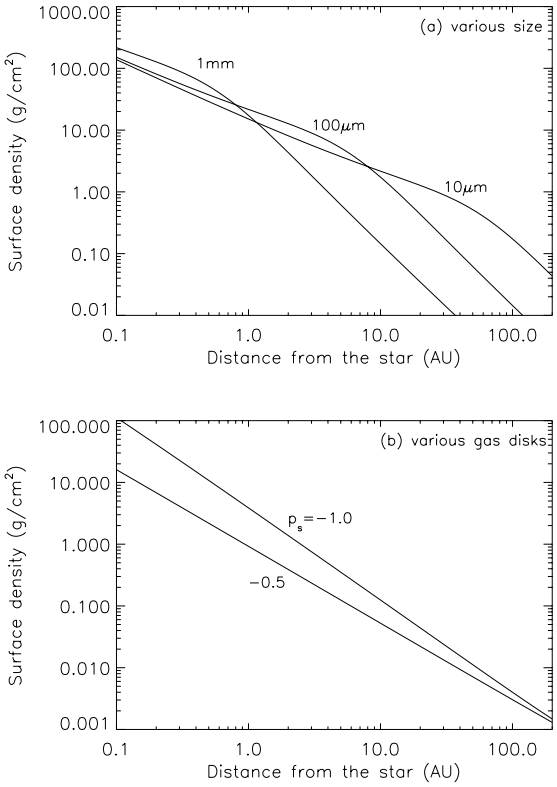

Fig. 9.— Surface density of dust disks, Σ_d. (a) The disk is composed of single sized particles of $s = 1$ mm, 100 μm, and 10 μm from the left line. The mass flux $\dot{M}_d$ is assumed to be $10^{-10} M_\odot$ yr^{-1}. (The mass flux of the gas is $10^{-8} M_\odot$ yr^{-1}.) The gas disk is the standard model ($p_s = -1.0$). (b) The disk is composed of particles with a power law size distribution. The indices of the surface density profiles of the gas disks are $p_s = -1.0$ and -0.5 from the upper line. The particle number flux is assumed to be proportional to $s^{-3.5}$. The minimum and maximum sizes of particles are 0.1 μm and 10 cm, respectively. The total mass flux is $\dot{M}_{d,\mathrm{all}} = 10^{-10} M_\odot$ yr^{-1}.